

Leveraging Motion Estimation for Efficient Bayer-Domain Computer Vision

Haichao Wang¹, Xinyue Xi¹, Jiangtao Wen², Yuxing Han¹

¹Shenzhen International Graduate School, Tsinghua University

²Department of Computer Science, New York University

Hychaowang@outlook.com, losea0602@gmail.com, jw9263@nyu.edu, yuxinghan@sz.tsinghua.edu.cn

Abstract

Existing computer vision processing pipeline acquires visual information using an image sensor that captures pixel information in the Bayer pattern. The raw sensor data are then processed using an image signal processor (ISP) that first converts Bayer pixel data to RGB on a pixel by pixel basis, followed by video convolutional network (VCN) processing on a frame by frame basis. Both ISP and VCN are computationally expensive with high power consumption and latency. In this paper, we propose a novel framework that eliminates the ISP and leverages motion estimation to accelerate video vision tasks directly in the Bayer domain. We introduce Motion Estimation-based Video Convolution (MEVC), which integrates sliding-window motion estimation into each convolutional layer, enabling prediction and residual-based refinement that reduces redundant computations across frames. This design bridges the structural gap between block-based motion estimation and spatial convolution, enabling accurate, low-cost processing. Our end-to-end pipeline supports raw Bayer input and achieves over 70% reduction in FLOPs with minimal accuracy degradation across video semantic segmentation, depth estimation, and object detection benchmarks, using both synthetic Bayer-converted and real Bayer video datasets. This framework generalizes across convolution-based models and marks the first effective reuse of motion estimation for accelerating video computer vision directly from raw sensor data.

Introduction

Video computer vision is a critical field within artificial intelligence, powering technologies from self-driving cars to advanced security systems. Although transformer-based models have shown remarkable progress, video convolutional networks (VCNs) (He et al. 2016; Yu et al. 2018; Long, Shelhamer, and Darrell 2015) maintain their lead in applications where computational resources are limited or real-time processing is required. Consequently, optimizing the efficiency of video computer vision systems in these constrained environments is a key area of focus.

The efficiency of video computer vision systems is hampered by bottlenecks at both the front-end and back-end. At the front-end, a computationally intensive Image Signal Processor (ISP) is required to convert raw Bayer data into the

RGB format pixel-by-pixel before feeding it to vision models. Subsequently, at the back-end, traditional frameworks process the high-resolution video frame by frame, failing to exploit inherent temporal redundancies. This approach leads to unnecessarily high computational complexity and latency.

To improve efficiency, researchers have studied video convolutional network acceleration (Kondratyuk et al. 2021; Li et al. 2019; Li, Shi, and Lin 2018) using two approaches. The first approach processes key frames and non-key frames with different models and performances, larger-scale models and higher performances for key frames, but smaller-scale models and lower performance for non-key frames (Jain, Wang, and Gonzalez 2019; Hu et al. 2023), with a compensation module to enhance vision performance for current frame outputs using information for key frames. For videos with limited scene changes, such schemes perform reasonably well, however, redundant calculations still exist. The second approach aimed at reducing temporal redundancy. For instance, BlockCopy (Verelst and Tuytelaars 2021) divides frames into blocks and uses a reinforcement learning model to decide whether a current frame block should be copied from the co-located block in the reference frame or processed by a standard model. By ignoring the differences between current and reference blocks, computer vision performance degrades rapidly as acceleration ratio increases.

The current paper proposes an efficient video computer vision framework to accelerate VCN-based computer vision without computer vision performance degradation. As shown in Figure 1, instead of converting Bayer videos into RGB videos for subsequent processing, we introduce a Bayer-format pipeline, which directly uses Bayer data so as to remove ISP from the pipeline. Bayer training and testing data were obtained using Invertible-ISP (Xing, Qian, and Chen 2021), an invertible convolutional network and a differentiable JPEG module. Then, we propose an efficient video convolution called Motion estimation-based Video Convolution (MEVC), where repeated and unnecessary convolution calculations are reduced by introducing motion estimation (ME) into the each convolutional layer. For each block in a current frame, motion estimation finds the most similar block in the reference frame, and records the corresponding motion vector and residual. The output of the current frame is then predicted from the reference frame with residual compensation using the motion vector (MV) and

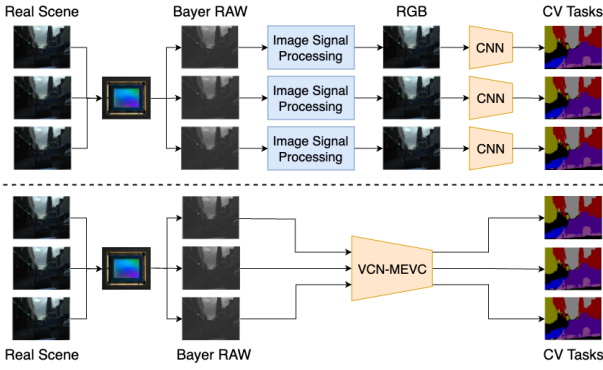


Figure 1: On the upper side is the traditional pipeline with image signal processor module. On the lower side is the our proposed efficient video computer vision framework with Bayer-format pipeline and motion estimation-based video convolution.

residual. Since the residual maps are sparse, the calculations for compensation are greatly reduced. The challenge in this approach lays fundamentally in the gap between motion estimation and convolution, which sliding-window motion estimation and compensation are designed to address. Our main contributions can be summarized as follows:

1. For the first time, introduce an efficient Motion estimation-based video convolution that is generic to different computer vision tasks and VCNs.
2. End-to-end Bayer-format pipeline for video computer vision, without ISP processing, thereby reducing complexity.
3. Sliding-window motion estimation and compensation for the efficient motion estimation-based video convolution.
4. Experimental results using various computer vision tasks and a variety of datasets, including public datasets and a self-collected Bayer-format dataset, demonstrate that our framework significantly accelerates video computer vision with minimal performance loss.

Related Works

Video Convolutional Network Acceleration

Video convolutional networks (VCNs) are widely used in video understanding tasks such as segmentation, detection, and depth estimation. However, their computational cost is high due to repeated processing of temporally similar frames. Prior works on VCN acceleration mainly fall into two categories.

The first category introduces temporal redundancy-aware scheduling (Hu et al. 2020). For example, Accel (Jain, Wang, and Gonzalez 2019) and AR-Seg (Hu et al. 2023) process key frames with a full model and interpolate non-key frames using lightweight models or low-resolution inputs, with feature-level fusion for compensation. While effective in low-motion scenarios, these methods often fail to adapt to varying motion levels and suffer from over-computation

on low-dynamic frames or degraded performance on high-motion ones.

The second category attempts to exploit frame-level redundancy more directly. BlockCopy (Verelst and Tuytelaars 2021) and TapLab(Feng et al. 2022) employ block-wise reuse of feature maps based on similarity, using learned or heuristic policies to determine when to copy or compute. However, these approaches typically omit residual compensation and are sensitive to alignment errors, leading to noticeable accuracy degradation under large or misaligned motion.

In contrast to both paradigms, our method introduces motion estimation directly into the convolutional layers, enabling fine-grained reuse of computation across frames with explicit residual correction. Unlike methods that reuse entire blocks or interpolate features, our approach decomposes convolution into motion-predicted outputs and sparse residual updates, maintaining accuracy while achieving higher compression.

Motion Estimation

Motion estimation (ME) is a fundamental component of video compression, where it enables predictive coding based on temporal redundancy. Despite its long history in video codecs, ME remains underutilized in deep learning-based computer vision pipelines. Recent efforts have applied ME-inspired techniques for object tracking, optical flow pre-processing (Dosovitskiy et al. 2015; Ilg et al. 2017; Sun et al. 2018), or compressed-domain inference. However, these methods treat motion estimation as an external module or a feature (Feng et al. 2022; Hu et al. 2023; Xiong et al. 2021), rather than a core operator. To our knowledge, our work is the first to integrate motion estimation as a differentiable, layer-wise primitive for accelerating video convolution. Furthermore, our proposed sliding-window motion estimation adapts classical block matching techniques to the structure of convolutional kernels, enabling compatibility with standard architectures while preserving high matching fidelity.

Bayer-Domain Vision

Most computer vision models assume RGB inputs preprocessed by image signal processors (ISPs). Recent works on inverse ISP learning or joint ISP-vision optimization have explored reducing this dependency, such as (Zhou et al. 2021) and (Xing, Qian, and Chen 2021). However, few attempt to eliminate ISP entirely. Our framework removes the ISP altogether, enabling end-to-end inference directly from raw Bayer sensor data. By combining ISP-free input processing with motion-compensated convolution, our method forms a unified, efficient pipeline for real-time Bayer-domain video vision.

Efficient Video Computer Vision Framework

We propose an end-to-end framework that eliminates the traditional image signal processor (ISP) and leverages motion estimation to accelerate video convolutional networks (VCNs) in the Bayer domain. Our approach is built on two

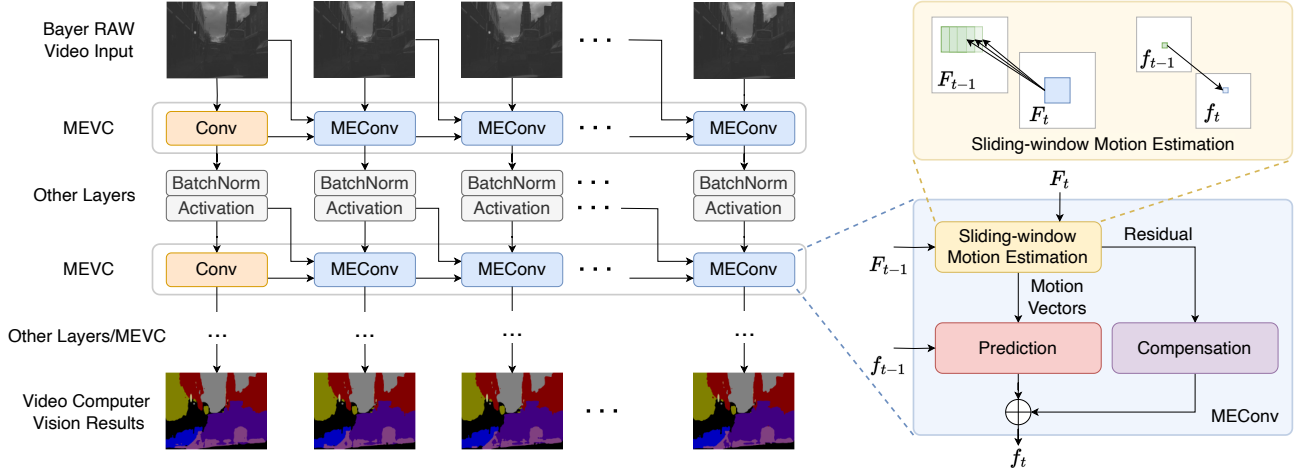


Figure 2: The diagram of our proposed framework. On the left is an overview of an example model, which receives Bayer RAW video as input and replaces standard convolution with our proposed MEVC modules. On the right is an overview MEConv module and sliding-window motion estimation module, which plays critical roles in the MEVC.

key components: a direct Bayer-format processing pipeline and a novel convolutional module called Motion Estimation-based Video Convolution (MEVC). The following sections describe each component in detail.

End-to-End Bayer-Domain Pipeline

Conventional computer vision pipelines rely on ISPs to convert raw Bayer sensor data into RGB images. This preprocessing is costly and non-differentiable. To bypass this bottleneck, we directly use Bayer data as input to the neural network and train all models in the Bayer domain. As illustrated in Figure 2, video convolutional operation is accelerated using sliding-window motion estimation to identify temporal correlation relationships between blocks in reference and current frames, as well as the residual map, followed by a compensation framework to correct the predict output based on the residual map. This design eliminates the computational overhead of ISP while preserving compatibility with standard video vision datasets and tasks.

Motion Estimation-based Video Convolution

To reduce redundant computation across temporally adjacent frames, we introduce motion estimation-based video convolution (MEVC) - a convolutional module that incorporates motion estimation directly into feature extraction. Each video sequence is divided into groups of pictures (GOPs). The first frame in each GOP is treated as a key frame and is processed using standard convolutions. For subsequent frames (non-key frames), we apply MEVC modules to reuse computation from previous frames.

In traditional video coding, ME is performed for each block in a current frame to find the best match block in the reference frame within a search range. As shown in Figure 3 (a), the position difference is recorded as Motion Vector (MV) and the block difference is recorded as Residual Map *Res*. During decoding process in Figure 3 (b), the cur-

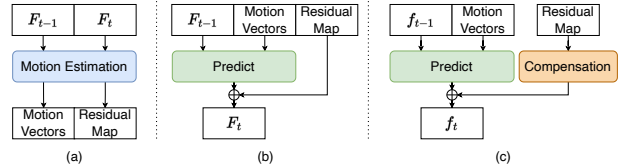


Figure 3: Figure (a) denotes the encode process with motion estimation while Figure (b) denotes the decode process. Figure (c) denotes the prediction and compensation of current frame results.

rent frame F_t is reconstructed by the motion vectors and the residual map from the reference frame F_{t-1} . This process can be expressed as

$$MV, Res = ME(F_{t-1}, F_t) \quad (1)$$

$$F_t = predict[F_{t-1}, MV] + Res \quad (2)$$

where F_{t-1} denotes the reference frame and F_t denotes the current frame.

Convolution is a linear operator, as shown in Figure 4, therefore equation 2 can be expressed as

$$Conv(F_t) = Conv[predict(F_{t-1}, MV)] + Conv(Res) \quad (3)$$

where $Conv$ denotes a convolutional operation. Because of the correspondence between the input blocks and the output pixels, equation 3 can be further transformed to

$$Conv(F_t) = predict[Conv(F_{t-1}, MV)] + Conv(Res) \quad (4)$$

where the $Conv(F_{t-1})$ is already known during the convolution over the reference frame, and residual map *Res* is usually sparse, as illustrated in Figure 3 (c). The above analysis can be generalized to features at different convolutional layers of a convolution network.

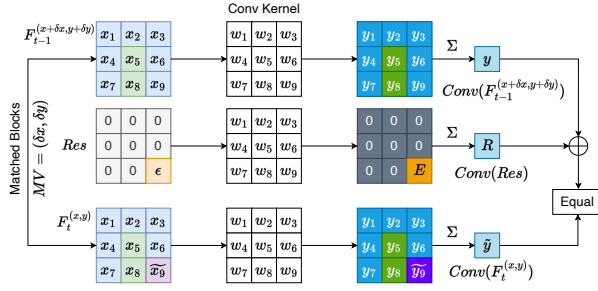


Figure 4: An example of the convolution’s linearity. The current frame block $F_t^{(x,y)}$ is decomposed into the matched reference frame block $F_{t-1}^{(x+\delta x, y+\delta y)}$ and a residual with slight difference ϵ , where $x_9 = x_9 + \epsilon$. After the convolution, the sum of the known $\text{Conv}(F_{t-1}^{(x+\delta x, y+\delta y)})$ and $\text{Conv}(\text{Res})$ equals to $\text{Conv}(F_t^{(x,y)})$.

On a higher level, as shown in Figure 2, the proposed MEVC contains two parts, a standard convolution and a proposed MEConv. The key frames are first processed by the standard convolution layer, whose output is then used as a reference by the next MEConv module. In MEConv module, the reference frame input F_{t-1} and the current frame input F_t are sent into sliding-window ME module, which produces motion vectors and residual maps. Features are predicted by the prediction module and compensated by the compensate module. At last, we replace the standard convolution with MEVC to obtain the final models.

Sliding-window Motion Estimation

In our proposed framework, we embed motion estimation directly into the convolutional layers to identify and leverage temporal redundancies, enabling significant reductions in redundant computation. However, a key challenge arises due to the structural mismatch between conventional block-based ME and the spatial organization of convolution operations in deep neural networks. Specifically, traditional ME uses large, non-overlapping blocks, whereas convolutional layers operate on overlapping patches (defined by stride) with small, often odd-sized kernels (e.g., 3×3) for symmetry.

To bridge this gap, we adopt a **sliding-window motion estimation strategy**, illustrated in Figure 5. In this formulation, the ME block size is matched to the convolution kernel size, and the search is performed in a sliding-window fashion across the input frame. The stride of the convolution is incorporated into the search mechanism, ensuring that each searched block corresponds to a unique output activation. This design aligns the spatial granularity of ME with that of the convolution operation, allowing end-to-end integration. During ME, the SAD criterion is used to identify the best-matching block from the previous reference frame. The residual between the current block and its match is computed and compared to a threshold τ ; any residual value below τ is suppressed to zero, promoting sparsity. To further reduce unnecessary computation, we introduce an **early-stopping**

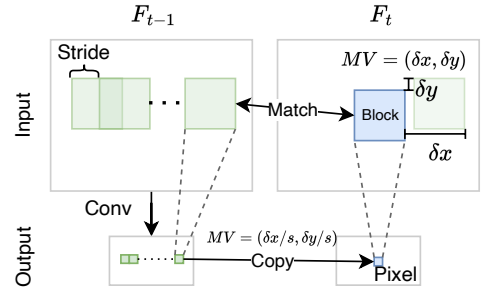


Figure 5: Sliding-window motion estimation aligned with convolutional output. Each output pixel corresponds to a matched input block determined via block-level SAD search.

mechanism: if the residual sparsity of a candidate match exceeds a predefined threshold (e.g., 0.3), the search is terminated early.

In the compensation step, we ensure alignment between predicted features and convolution outputs. Because the convolution stride alters the spatial resolution of feature maps, we scale the motion vectors by the stride factor s before applying them. The predicted feature at location $(x/s, y/s)$ in the current frame is computed as:

$$f_t^{x/s, y/s} = f_{t-1}^{(x+\delta x/s)/s, (y+\delta y/s)/s} \quad (5)$$

where $(x/s, y/s)$ represents the output pixel coordinate, and $(\delta x/s, \delta y/s)$ denotes the stride-normalized motion vector. The final output is obtained by combining the motion-compensated prediction and the convolution of the residual:

$$\hat{f}_t = \text{Pred} + \text{Conv}(\text{Res})$$

Moreover, the residual map R exhibits high spatial redundancy, which we exploit to skip convolution on zero-valued or near-zero patches, further reducing computation.

Acceleration Analysis

Assume the input data with shape (C_{in}, H_{in}, W_{in}) is processed through a 2D convolution layer with C_{out} filters, a kernel size of k , a stride of s , resulting in an output shape of $(C_{out}, H_{out}, W_{out})$. The computational complexity for standard convolution is

$$\text{FLOPs}_{\text{Conv}} = 2k^2 C_{in} C_{out} H_{out} W_{out}.$$

For ME, suppose the matching success ratio is called match ratio α and the sparsity of residual map is recorded as β . The number of addition and multiplication operations is

$$\text{FLOPs}_{\text{ME}} = \frac{2k^2 C_{in} H_{out} W_{out} (2R + 1)^2}{s^2}.$$

The computational cost of the convolution for the unmatched blocks is

$$\text{FLOPs}_{\text{unmatched}} = (1 - \alpha) \text{Conv}_{\text{ops}},$$

The computation of the convolution over the residual map:

$$\text{FLOPs}_{\text{Res}} = \alpha\beta\text{Conv}_{\text{ops}}$$

As a result, the overall computation of our framework is:

$$\text{FLOPs}_{\text{MEVC}} = \text{FLOPs}_{\text{ME}} + \text{FLOPs}_{\text{Unmatched}} + \text{FLOPs}_{\text{Res}}$$

The acceleration ratio is:

$$\text{Acceleration} = \alpha - \alpha\beta - \frac{(2R + 1)^2}{s^2 C_{\text{out}}}$$

where the *Acceleration* denotes the reduction ratio relative to standard convolution, considering both addition and multiplication operations. Typically, the match ratio α is high and the sparsity β is low, which results in a high acceleration ratio. Moreover, the overall acceleration of the proposed framework needs to take the removal of ISP into consideration.

In our experiments, ME was implemented using the CUDA (Luebke 2008) (Compute Unified Device Architecture) framework. We do not report wall-clock time comparisons due to a fundamental mismatch in implementation: the baseline convolutions benefit from highly optimized GPU libraries (e.g., CUTLASS), whereas our motion estimation (ME) module is a custom CUDA implementation lacking comparable low-level optimization. A direct runtime comparison would therefore reflect the maturity of library support rather than the algorithmic efficiency itself. To ensure a hardware-agnostic and fair evaluation, we focus on FLOPs as our primary metric, which directly measures the theoretical reduction in computational complexity. We acknowledge that our current ME implementation can be further optimized.

Experiments

Experimental Setup

We evaluate the proposed framework across three representative computer vision tasks: video semantic segmentation, video depth estimation, and video object detection. Our method is designed to be compatible with standard convolution-based backbones, enabling broad applicability across task domains.

Semantic Segmentation. We conduct experiments on two widely used benchmarks: CamVid (Brostow et al. 2008; Brostow, Fauqueur, and Cipolla 2008) and Cityscapes (Cordts et al. 2016). CamVid consists of over 700 densely annotated frames from urban driving sequences spanning 10 minutes, with 32 semantic categories. Cityscapes provides 5,000 finely annotated and 20,000 coarsely labeled images of urban street scenes. We integrate our framework into two popular convolutional backbones: PSPNet (Zhao et al. 2017) and HRNet (Wang et al. 2020), and evaluate their performance in the Bayer domain using our motion-aware formulation.

Depth Estimation. For monocular depth prediction, we adopt the NYU-Depth V2 dataset (Nathan Silberman and Fergus 2012), which contains 101,377 RGB-D image pairs for training and 1,308 pairs for evaluation. We implement

our framework using the fully convolutional architecture of Hu et al. (Hu et al. 2019) as the backbone and adapt it for raw Bayer input using our MEVC-based pipeline.

Object Detection. For video object detection, we use the large-scale ImageNet-VID dataset (Russakovsky et al. 2015), which includes over 1 million annotated frames for training and more than 100,000 frames for validation. We employ RetinaNet (Lin et al. 2017) as the backbone and apply our motion-compensated convolution module to reduce temporal redundancy during inference.

Bayer Domain Conversion and Real-World Data. For all public datasets, the original RGB frames are converted to Bayer-format raw inputs using the Invertible-ISP model. To further validate real-world applicability, we construct a custom dataset, **CityBayer**, by capturing raw video from industrial cameras under diverse lighting and motion conditions. CityBayer provides native Bayer-domain sequences without any ISP post-processing. Due to the difficulty of pixel-level annotation on raw sensor data, we use this dataset solely for inference-based evaluation.

Experiments Results

Video Semantic Segmentation We evaluate the proposed MEVC-based acceleration framework on video semantic segmentation using two widely adopted CNN backbones: PSPNet18 and HRNet-W48. Experiments are conducted on two benchmark datasets: CamVid and Cityscapes. Performance is measured in terms of mean Intersection over Union (mIoU), which reflects segmentation accuracy, and Giga Floating-point Operations (GFLOPs), representing computational cost.

As shown in Table 1, our framework achieves segmentation performance comparable to traditional RGB-based models, despite operating directly on raw Bayer data and utilizing motion-aware convolution to reduce computation. For example, on the Cityscapes dataset with HRNet-W48, our method achieves an mIoU of 78.98%, nearly identical to its RGB counterpart. At the same time, MEVC delivers substantial acceleration, with GFLOPs reduced by approximately 70% for both PSPNet18 and HRNet-W48.

Table 2 compares our method with existing acceleration approaches. While previous methods like Accel and AR-Seg apply uniform processing to all frames—leading to inefficient use of compute in low-motion scenarios, our method adapts to temporal redundancy using predictive convolution with motion compensation. Other approaches, such as BlockCopy and TapLab, yield higher FLOPs savings but at the cost of significant accuracy degradation (6.7% and 4.1%, respectively). In contrast, our framework achieves over 70% reduction in FLOPs with minimal loss in segmentation accuracy.

Notably, the computational savings reported exclude ISP processing cost, which is required for all RGB-domain methods but eliminated in our pipeline. Prior work estimates ISP complexity to range from 1 GFLOP (conventional) to over 100 GFLOPs (learned ISP networks) (Mei et al. 2019; Liang et al. 2021; Ratnasingam 2019), suggesting our reported efficiency gains are conservative.

Table 1: Results of our framework deployed on PSPNet18 and HRNet-W48, with GOP of 12, threshold of 0.01 and search range of 1.

| Method | PSPNet18 | | HRNet-W48 | |
|---------------------------|----------|--------|-----------|--------|
| | mIoU(%) | GFLOPs | mIoU(%) | GFLOPs |
| CamVid Dataset | | | | |
| RGB | 69.43 | 309.02 | 75.48 | 247.30 |
| Bayer | 69.27 | 308.82 | 75.67 | 247.10 |
| Ours | 69.28 | 90.85 | 75.67 | 170.89 |
| Cityscapes Dataset | | | | |
| RGB | 69.00 | 560.97 | 79.06 | 748.68 |
| Bayer | 69.11 | 560.37 | 78.98 | 748.08 |
| Ours | 69.10 | 166.52 | 78.98 | 228.91 |

To further validate our method under real-world sensor conditions, we test on five Bayer-domain clips from the CityBayer dataset, captured with industrial cameras. Under a GOP size of 12, search range of 1, and threshold of 0.01, the observed GFLOPs reductions are 72.18%, 73.60%, 73.01%, 72.24%, and 72.68%, respectively. These results confirm the robustness and generalizability of our approach across synthetic and real Bayer data.

Table 2: Performance comparison with previous works on the CamVid and Cityscapes datasets.

| | Method | mIoU (%) | GFLOPs | Δ FLOPs (%) |
|------------|--------------------------|----------|---------|--------------------|
| CamVid | PSPNet | 69.43 | 309.02 | — |
| | Accel-DL18 | 66.15 | 397.70 | +61.9 |
| | TD ⁴ -PSP18 | 70.13 | 363.70 | +17.7 |
| | BlockCopy | 66.75 | 107.52 | -45.7 |
| | TapLab-BL2 | 67.57 | 117.73 | -50.2 |
| | Jain et al. | 67.61 | 146.97 | -53.8 |
| | AR ^{0.6} -PSP18 | 70.82 | 101.98 | -57.0 |
| | Ours-PSP18 | 69.28 | 90.85 | -70.6 |
| Cityscapes | PSPNet | 69.00 | 560.97 | — |
| | Accel-DL18 | 68.25 | 1011.75 | +96.0 |
| | TD ⁴ -PSP18 | 70.11 | 673.06 | +20.0 |
| | BlockCopy | 67.69 | 294.20 | -41.2 |
| | TapLab-BL2 | 68.90 | 237.29 | -50.6 |
| | Jain et al. | 68.57 | 342.67 | -52.5 |
| | AR ^{0.6} -PSP18 | 69.45 | 234.91 | -58.1 |
| | Ours-PSP18 | 69.10 | 166.52 | -70.3 |

Video Depth Estimation We evaluate the effectiveness of our proposed MEVC framework on video depth estimation using the NYU-Depth V2 dataset and the real-world CityBayer dataset. Depth prediction performance is assessed using two standard metrics: Root Mean Squared Error (RMSE) and Mean Relative Error (REL).

On the NYU-Depth dataset, we first convert the RGB inputs to Bayer format using the Invertible-ISP model. Our

approach achieves a significant computational reduction of 71.33% in FLOPs, while maintaining accuracy within 0.1% deviation in both RMSE and REL compared to the full-resolution RGB baseline. This highlights the efficiency of our motion-aware, reconstruction-free framework in preserving depth estimation fidelity under strong acceleration.

To further validate generalization to real Bayer-domain input, we test our framework on the CityBayer dataset captured using industrial-grade cameras. Across multiple video clips, the average reduction in computational cost reaches 73.14%, further confirming the practical benefits of our approach in real-world scenarios.

Video Object Detection We assess the performance of our MEVC-based framework on the video object detection task using the ImageNet-VID dataset and our real-world CityBayer dataset. Detection accuracy is evaluated using Average Precision (AP), while computational efficiency is measured by FLOPs.

On the Bayer-format version of ImageNet-VID, generated via the Invertible-ISP model, our approach achieves a substantial reduction of 70.48% in FLOPs with less than 0.1% degradation in AP. This result demonstrates that our method can effectively accelerate object detection without compromising performance.

When applied to the CityBayer dataset, which contains native raw Bayer video captured using industrial sensors, our framework achieves an average computational reduction of 72.56%. These findings highlight the robustness and applicability of MEVC for real-world object detection scenarios involving raw sensor inputs.

Discussions on Parameters

Group of Pictures (GOP) Length. We define the Group of Pictures (GOP) in a manner analogous to traditional video coding. Specifically, a GOP consists of a sequence of frames beginning with a reference (key) frame, followed by a set of non-key frames up to (but not including) the next reference frame. In our system, the reference frame is fully processed using conventional convolution, while the subsequent non-key frames are handled using motion-compensated prediction and residual refinement via MEVC.

To examine the effect of GOP size on acceleration and performance, we conduct experiments across a range of GOP lengths. As shown in Table 3, the overall computational savings generally increase with longer GOPs. This trend arises because more non-key frames are introduced per reference frame, allowing a larger portion of the video to benefit from motion-based acceleration. However, the marginal gain in acceleration diminishes beyond a certain GOP length, due to the increasing temporal distance between non-key frames and their reference, which reduces motion correlation and prediction accuracy.

Threshold. The residual threshold is a critical hyperparameter that governs the sparsity of MEVC’s residual update. Specifically, it determines which residual values are considered negligible and thus omitted from further computation. A higher threshold results in more aggressive filtering

Table 3: Acceleration under different GOP lengths.

| GOP length | GFLOPs | Δ FLOPs (%) |
|------------|--------|--------------------|
| 2 | 334.45 | -40.4 |
| 4 | 233.82 | -58.3 |
| 6 | 200.13 | -64.3 |
| 8 | 183.06 | -67.4 |
| 10 | 173.07 | -69.2 |
| 12 | 166.52 | -70.3 |

of small residuals, reducing the number of pixels processed and thereby improving computational efficiency.

Table 4 presents the relationship between threshold values, FLOPs reduction, and segmentation accuracy (mIoU). As the threshold increases, FLOPs decrease due to fewer residual computations. Notably, when the threshold is set below 0.01, the performance loss remains minimal while computation drops significantly. However, beyond a threshold of 0.05, additional FLOPs savings plateau while the mIoU begins to degrade more noticeably. This suggests that the majority of residual noise lies below the 0.01 level, and overly aggressive thresholding risks discarding informative signal in the residual map.

Table 4: Acceleration under different thresholds.

| Threshold | mIoU (%) | GFLOPs | Δ FLOPs (%) |
|-----------|----------|--------|--------------------|
| 0 | -0.00 | 325.09 | -41.9 |
| 0.01 | -0.01 | 166.52 | -70.3 |
| 0.05 | -2.94 | 74.11 | -86.8 |
| 0.1 | -3.26 | 71.67 | -87.2 |

Search Range. The search range defines the spatial extent over which motion estimation is performed for each output feature. In our framework, motion vectors are computed by exhaustively comparing candidate blocks within this range to identify the best match. We evaluate the effect of varying the search range from 1 to 3 while holding the residual threshold constant at 0.01.

As shown in the results, a search range of 1 yields the most efficient configuration, requiring only 166.52 GFLOPs and achieving a 70.3% reduction in computation. Increasing the search range to 2 raises the computational cost to 186.47 GFLOPs, with the FLOPs reduction falling to 66.7%. At a search range of 3, the GFLOPs further increase to 219.08, with a diminished reduction of just 60.9%. This trend reflects the quadratic complexity of the exhaustive block matching algorithm used in our ME module, where the number of candidate comparisons grows rapidly with the size of the search window. Overall, a search range of 1 offers a strong trade-off between accuracy and computational efficiency. Larger ranges yield diminishing returns in performance but incur significant increases in processing cost, making them less practical for real-time or resource-constrained deployments.

Ablation Study

To demonstrate the effectiveness of each component in our framework, acceleration and segmentation performance were both tested under different settings as follows:

1. Use PSPNet to process all frames in Bayer videos.
2. Process Videos with MEVC without the compensation.
3. Process Videos with MEVC with the compensation, but without the threshold.
4. Process Videos with MEVC with the compensation and the threshold.

Table 5: Acceleration and performance under different settings.

| Setting | mIoU (%) | GFLOPs | Δ FLOPs (%) |
|---------|----------|--------|--------------------|
| 1 | 69.11 | 560.97 | -0.00 |
| 2 | 41.74 | 72.41 | -87.1 |
| 3 | 69.11 | 325.09 | -41.9 |
| 4 | 69.10 | 166.52 | -71.3 |

The results are given in Table 5. The convolution of the residual maps as compensation is the main computation of the non-key frames. When removing the compensation, the computation greatly reduces but the semantic segmentation performance is significantly impacted. Under setting 3, the performance became lossless, which proved the effectiveness and necessity of the compensation. However, the setting 3 required much more computation than setting 4 while maintaining nearly the same semantic segmentation performance, due to noise in residual maps that should not be calculated and had no influence on the final performance but costed a lot of computation. This finding proves that the threshold was set reasonably.

Conclusion

We present a unified framework that rethinks the design of video computer vision systems by eliminating the ISP and integrating motion estimation directly into the convolutional process. By operating on raw Bayer data and introducing Motion Estimation-based Video Convolution (MEVC), our method effectively reduces redundant computation through motion-compensated prediction and sparse residual refinement. A sliding-window alignment strategy bridges the gap between block-based motion estimation and convolutional feature extraction, enabling seamless integration into standard CNN backbones. Experiments across semantic segmentation, depth estimation, and object detection demonstrate that our approach achieves over 70% FLOPs reduction with minimal performance loss. This framework is in general functional for all convolution-based neural networks and downstream tasks.

References

Brostow, G. J.; Fauqueur, J.; and Cipolla, R. 2008. Semantic Object Classes in Video: A High-Definition Ground Truth Database. *Pattern Recognition Letters*, xx(x): xx–xx.

Brostow, G. J.; Shotton, J.; Fauqueur, J.; and Cipolla, R. 2008. Segmentation and Recognition Using Structure from Motion Point Clouds. In *ECCV (I)*, 44–57.

Cordts, M.; Omran, M.; Ramos, S.; Rehfeld, T.; Enzweiler, M.; Benenson, R.; Franke, U.; Roth, S.; and Schiele, B. 2016. The cityscapes dataset for semantic urban scene understanding. In *Proceedings of the IEEE conference on computer vision and pattern recognition*, 3213–3223.

Dosovitskiy, A.; Fischer, P.; Ilg, E.; Hausser, P.; Hazirbas, C.; Golkov, V.; Van Der Smagt, P.; Cremers, D.; and Brox, T. 2015. Flownet: Learning optical flow with convolutional networks. In *Proceedings of the IEEE international conference on computer vision*, 2758–2766.

Feng, J.; Li, S.; Li, X.; Wu, F.; Tian, Q.; Yang, M.-H.; and Ling, H. 2022. TapLab: A Fast Framework for Semantic Video Segmentation Tapping Into Compressed-Domain Knowledge. *IEEE Transactions on Pattern Analysis and Machine Intelligence*, 44(3): 1591–1603.

He, K.; Zhang, X.; Ren, S.; and Sun, J. 2016. Deep residual learning for image recognition. In *Proceedings of the IEEE conference on computer vision and pattern recognition*, 770–778.

Hu, J.; Ozay, M.; Zhang, Y.; and Okatani, T. 2019. Revisiting single image depth estimation: Toward higher resolution maps with accurate object boundaries. In *2019 IEEE winter conference on applications of computer vision (WACV)*, 1043–1051. IEEE.

Hu, P.; Caba, F.; Wang, O.; Lin, Z.; Sclaroff, S.; and Perazzi, F. 2020. Temporally distributed networks for fast video semantic segmentation. In *Proceedings of the IEEE/CVF Conference on Computer Vision and Pattern Recognition*, 8818–8827.

Hu, Y.; He, Y.; Li, Y.; Li, J.; Han, Y.; Wen, J.; and Liu, Y.-J. 2023. Efficient Semantic Segmentation by Altering Resolutions for Compressed Videos. In *2023 IEEE/CVF Conference on Computer Vision and Pattern Recognition (CVPR)*, 22627–22637. Vancouver, BC, Canada: IEEE. ISBN 9798350301298.

Ilg, E.; Mayer, N.; Saikia, T.; Keuper, M.; Dosovitskiy, A.; and Brox, T. 2017. Flownet 2.0: Evolution of optical flow estimation with deep networks. In *Proceedings of the IEEE conference on computer vision and pattern recognition*, 2462–2470.

Jain, S.; Wang, X.; and Gonzalez, J. E. 2019. Accel: A Corrective Fusion Network for Efficient Semantic Segmentation on Video. In *2019 IEEE/CVF Conference on Computer Vision and Pattern Recognition (CVPR)*, 8858–8867. Long Beach, CA, USA: IEEE. ISBN 978-1-72813-293-8.

Kondratyuk, D.; Yuan, L.; Li, Y.; Zhang, L.; Tan, M.; Brown, M.; and Gong, B. 2021. Movinets: Mobile video networks for efficient video recognition. In *Proceedings of the IEEE/CVF conference on computer vision and pattern recognition*, 16020–16030.

Li, H.; Xiong, P.; Fan, H.; and Sun, J. 2019. Dfanet: Deep feature aggregation for real-time semantic segmentation. In *Proceedings of the IEEE/CVF conference on computer vision and pattern recognition*, 9522–9531.

Li, Y.; Shi, J.; and Lin, D. 2018. Low-latency video semantic segmentation. In *Proceedings of the IEEE conference on Computer Vision and Pattern Recognition*, 5997–6005.

Liang, Z.; Cai, J.; Cao, Z.; and Zhang, L. 2021. Cameranet: A two-stage framework for effective camera isp learning. *IEEE Transactions on Image Processing*, 30: 2248–2262.

Lin, T.-Y.; Goyal, P.; Girshick, R.; He, K.; and Dollár, P. 2017. Focal loss for dense object detection. In *Proceedings of the IEEE international conference on computer vision*, 2980–2988.

Long, J.; Shelhamer, E.; and Darrell, T. 2015. Fully convolutional networks for semantic segmentation. In *Proceedings of the IEEE conference on computer vision and pattern recognition*, 3431–3440.

Luebke, D. 2008. CUDA: Scalable parallel programming for high-performance scientific computing. In *2008 5th IEEE international symposium on biomedical imaging: from nano to macro*, 836–838. IEEE.

Mei, K.; Li, J.; Zhang, J.; Wu, H.; Li, J.; and Huang, R. 2019. Higher-resolution network for image demosaicing and enhancing. In *2019 ieee/cvf international conference on computer vision workshop (iccvw)*, 3441–3448. IEEE.

Nathan Silberman, P. K., Derek Hoiem; and Fergus, R. 2012. Indoor Segmentation and Support Inference from RGBD Images. In *ECCV*.

Ratnasingam, S. 2019. Deep camera: A fully convolutional neural network for image signal processing. In *Proceedings of the IEEE/CVF International Conference on Computer Vision Workshops*, 0–0.

Russakovsky, O.; Deng, J.; Su, H.; Krause, J.; Satheesh, S.; Ma, S.; Huang, Z.; Karpathy, A.; Khosla, A.; Bernstein, M.; Berg, A. C.; and Fei-Fei, L. 2015. ImageNet Large Scale Visual Recognition Challenge. *International Journal of Computer Vision (IJCV)*, 115(3): 211–252.

Sun, D.; Yang, X.; Liu, M.-Y.; and Kautz, J. 2018. Pwcnnet: Cnns for optical flow using pyramid, warping, and cost volume. In *Proceedings of the IEEE conference on computer vision and pattern recognition*, 8934–8943.

Verelst, T.; and Tuytelaars, T. 2021. BlockCopy: High-Resolution Video Processing with Block-Sparse Feature Propagation and Online Policies. In *2021 IEEE/CVF International Conference on Computer Vision (ICCV)*, 5138–5147. Montreal, QC, Canada: IEEE. ISBN 978-1-66542-812-5.

Wang, J.; Sun, K.; Cheng, T.; Jiang, B.; Deng, C.; Zhao, Y.; Liu, D.; Mu, Y.; Tan, M.; Wang, X.; et al. 2020. Deep high-resolution representation learning for visual recognition. *IEEE transactions on pattern analysis and machine intelligence*, 43(10): 3349–3364.

Xing, Y.; Qian, Z.; and Chen, Q. 2021. Invertible image signal processing. In *Proceedings of the IEEE/CVF conference on computer vision and pattern recognition*, 6287–6296.

Xiong, J.; Po, L.-M.; Yu, W.-Y.; Zhao, Y.; and Cheung, K.-W. 2021. Distortion map-guided feature rectification for efficient video semantic segmentation. *IEEE Transactions on Multimedia*, 25: 1019–1032.

Yu, C.; Wang, J.; Peng, C.; Gao, C.; Yu, G.; and Sang, N. 2018. Bisenet: Bilateral segmentation network for real-time semantic segmentation. In *Proceedings of the European conference on computer vision (ECCV)*, 325–341.

Zhao, H.; Shi, J.; Qi, X.; Wang, X.; and Jia, J. 2017. Pyramid scene parsing network. In *Proceedings of the IEEE conference on computer vision and pattern recognition*, 2881–2890.

Zhou, W.; Zhang, X.; Wang, H.; Gao, S.; and Lou, X. 2021. Raw bayer pattern image synthesis for computer vision-oriented image signal processing pipeline design. *arXiv preprint arXiv:2110.12823*.